Design of robust differential microphone arrays with orthogonal polynomials

Chao Pan, Jacob Benesty, and Jingdong Chen

Citation: The Journal of the Acoustical Society of America **138**, 1079 (2015); doi: 10.1121/1.4927690
View online: https://doi.org/10.1121/1.4927690
View Table of Contents: https://asa.scitation.org/toc/jas/138/2
Published by the Acoustical Society of America

Design of robust differential microphone arrays with orthogonal polynomials

Chao Pan
Center of Intelligent Acoustics and Immersive Communications, Northwestern Polytechnical University, 127 Youyi West Road, Xi'an, Shaanxi 710072, China

Jacob Benesty
INRS-EMT, University of Quebec, 800 de la Gauchetiere Ouest, Suite 6900, Montreal, Quebec H5A 1K6, Canada

Jingdong Chen[a)]
Center of Intelligent Acoustics and Immersive Communications, Northwestern Polytechnical University, 127 Youyi West Road, Xi'an, Shaanxi 710072, China

(Received 17 March 2015; revised 11 July 2015; accepted 18 July 2015; published online 21 August 2015)

Differential microphone arrays have the potential to be widely deployed in hands-free communication systems thanks to their frequency-invariant beampatterns, high directivity factors, and small apertures. Traditionally, they are designed and implemented in a multistage way with uniform linear geometries. This paper presents an approach to the design of differential microphone arrays with orthogonal polynomials, more specifically with Jacobi polynomials. It first shows how to express the beampatterns as a function of orthogonal polynomials. Then several differential beamformers are derived and their performance depends on the parameters of the Jacobi polynomials. Simulations show the great flexibility of the proposed method in terms of designing any order differential microphone arrays with different beampatterns and controlling white noise gain. © *2015 Acoustical Society of America*. [http://dx.doi.org/10.1121/1.4927690]

[MRB] Pages: 1079–1089

I. INTRODUCTION

Microphone arrays have been intensively studied for processing audio and speech signals in acoustic environments. Because audio and speech signals are broadband in nature and their frequencies range from a few hertz to more than 20 kHz, it is necessary for the arrays to have uniform spatial responses at different frequencies; otherwise, distortion is added to either the signal of interest or noise, resulting in disturbing artifacts at the arrays' output (Ward *et al.*, 1998). Significant efforts have been devoted to the design of microphone arrays with uniform spatial responses over the last two decades. Many methods have been developed that can be broadly classified into three categories: nested arrays, broadband beamforming, and differential beamforming with differential microphone arrays (DMAs).

A nested array consists of a few subarrays with each operating at a small frequency range (Elko and Meyer, 2008; Chou, 1995). By adjusting the number of sensors and the spacing in each subarray, the global array can be controlled to have a constant beamwidth over the entire frequency range of interest. Although it is possible to achieve a constant beamwidth, a nested array generally requires a large number of microphones and a large array geometry. Another way to achieve constant beamwidth is through narrowband decomposition, leading to the so-called broadband beamforming (Doclo and Moonen, 2003; Benesty *et al.*, 2007; Elko and Meyer, 2008). Basically, the array signals are decomposed into multiple subbands. A narrowband beamformer is then designed in each subband with a constraint applied to control the beamwidth so that all the beamformers from different subbands can have the same beamwidth. Although it can make constant beamwidth across a wide range of frequencies, this way of broadband beamforming suffers from two prominent drawbacks: (1) the resulting beampatterns, particularly the sidelobes, still vary significantly from one frequency to another, which can cause tremendous distortion to the background and noise signals, and (2) it sacrifices the array gain at high frequencies.

In comparison, differential beamforming is perhaps the only approach so far that can achieve frequency-invariant beampatterns. Furthermore differential beamforming can achieve the maximal directional gains given the number of microphones and with a small DMA aperture (Elko and Meyer, 2008; Benesty and Chen, 2012). As a result, this type of beamforming has attracted much attention recently. Differential beamformers can be designed in a multistage manner (Elko and Meyer, 2008) or by solving a linear system determined by the nulls in the desired DMA beampattern (Benesty and Chen, 2012). It is well known that differential beamforming is sensitive to the sensors' location perturbations and other errors in the array system (Buck, 2002). In Benesty and Chen (2012), a null-constrained approach is developed to the design of robust differential beamformers by increasing the number of sensors for a fixed DMA order and exploiting the redundancy to maximize the

[a)]Electronic mail: jingdongchen@ieee.org

white noise gain (WNG). In Chen *et al.* (2014), a similar approach with nulls with multiplicity of more than one is presented.

Another way to design DMAs is by approximating the beampattern of the beamformer with some series expansions where the basic idea started with circular and spherical eigenbeamforming (Mathews and Zoltowski, 1994; Meyer, 2001; Rafaely, 2005; Yan *et al.*, 2011). Some initial work has already been presented recently, for example, in Zhao *et al.* (2014), where DMAs are designed using the MacLaurin's series approximation. In this paper, we propose a general way to design DMAs with orthogonal polynomials, which is more general than the early works in Zhao *et al.* (2014). We will show that the proposed design methods have more flexibility in compromising among WNG, directivity factor (DF), and frequency-invariant beampattern.

The organization of this paper is as follows. In Sec. II, we present the signal model and some important definitions. In Sec. III, we show how to express the beampatterns with orthogonal polynomials. In Sec. IV, we derive four DMA beamforming filters: non-robust, robust, constant beampattern (CP), and regularized CP. In Sec. V, we present the Jacobi polynomials and the corresponding properties. In Sec. VI, we evaluate the performance of the filters developed with the Jacobi polynomials. Finally, some conclusions are presented in Sec. VII.

II. SIGNAL MODEL, PROBLEM FORMULATION, AND DEFINITIONS

A. Signal model

We consider a farfield desired source signal that propagates from the azimuth angle, θ, in an anechoic acoustic environment at the speed of sound, i.e., $c = 340$ m/s, and impinges on a uniform linear array consisting of M omnidirectional microphones. The angular frequency is denoted by $\omega = 2\pi f$, where $f > 0$ is the temporal frequency. In this context, if we neglect the relative propagation loss from the source to the different microphones, the observation signal vector of length M can be expressed in the frequency domain as (Benesty *et al.*, 2008)

$$\begin{aligned}\mathbf{y}(\omega) &= [\,Y_1(\omega) \quad Y_2(\omega) \quad \cdots \quad Y_M(\omega)\,]^T \\ &= \mathbf{x}(\omega) + \mathbf{v}(\omega) \\ &= \mathbf{d}(\omega, \cos\theta)X(\omega) + \mathbf{v}(\omega),\end{aligned} \tag{1}$$

where $Y_m(\omega)$ is the mth microphone signal, the superscript ^{T} is the transpose operator, $\mathbf{x}(\omega) = \mathbf{d}(\omega, \cos\theta)X(\omega)$, $X(\omega)$ is the desired source signal, $\mathbf{v}(\omega)$ is the additive noise signal vector,

$$\mathbf{d}(\omega, \cos\theta) = [\,1 \quad e^{-\mathrm{i}\omega\tau_0\cos\theta} \quad \cdots \quad e^{-\mathrm{i}(M-1)\omega\tau_0\cos\theta}\,]^T \tag{2}$$

is the phase-delay vector of length M (its form is the same as the steering vector used in traditional beamforming), $\mathrm{i} = \sqrt{-1}$ is the imaginary unit, and $\tau_0 = \delta/c$ is the delay between two successive sensors at the angle $\theta = 0$, with δ being the interelement spacing.

To ensure that differential beamforming takes place, the following two assumptions are made (Elko, 2000; Elko and Meyer, 2008; Benesty and Chen, 2012):

(1) The sensor spacing, δ, is much smaller than the acoustic wavelength, $\lambda = c/f$, i.e., $\delta \ll \lambda$ (this implies that $\omega\tau_0 \ll 2\pi$). This assumption is required so that the true acoustic pressure differentials can be approximated by finite differences of the microphones' outputs.
(2) The desired source signal propagates from the angle $\theta = 0°$ (endfire direction). Therefore Eq. (1) becomes

$$\mathbf{y}(\omega) = \mathbf{d}(\omega, 1)X(\omega) + \mathbf{v}(\omega), \tag{3}$$

and, at the endfire, the value of the beamformer's beampattern should always be equal to 1 (or maximal).

B. Problem of beamforming

Beamforming is a process to estimate the desired signal, $X(\omega)$, from the array observations, $\mathbf{y}(\omega)$, given in Eq. (1) through linear filtering (Benesty *et al.*, 2008), i.e.,

$$\begin{aligned}Z(\omega) &= \sum_{m=1}^{M} H_m^*(\omega)Y_m(\omega) \\ &= \mathbf{h}^H(\omega)\mathbf{y}(\omega) \\ &= \mathbf{h}^H(\omega)\mathbf{d}(\omega, 1)X(\omega) + \mathbf{h}^H(\omega)\mathbf{v}(\omega),\end{aligned} \tag{4}$$

where $Z(\omega)$ is the estimate of the desired signal, $X(\omega)$,

$$\mathbf{h}(\omega) = [\,H_1(\omega) \quad H_2(\omega) \quad \cdots \quad H_M(\omega)\,]^T \tag{5}$$

is a complex-valued linear filter applied to the observation signal vector, $\mathbf{y}(\omega)$, and the superscripts * and H denote complex conjugation and conjugate-transpose, respectively. In our context, the distortionless constraint is desired. So we should have

$$\mathbf{h}^H(\omega)\mathbf{d}(\omega, 1) = 1. \tag{6}$$

The objective of beamforming is to find an optimal beamforming filter, $\mathbf{h}(\omega)$, under some criteria so that $Z(\omega)$ is a good estimate of $X(\omega)$.

C. Important definitions of performance measures

Signal-to-noise ratio (SNR) is one of the most important measures of the goodness of a beamformer. If we take microphone 1 as the reference and assume that the variances of all the sensors' noises are the same, we can define the input signal-to-noise ratio (iSNR) as

$$\mathrm{iSNR}(\omega) = \frac{\phi_X(\omega)}{\phi_{V_1}(\omega)}, \tag{7}$$

where $\phi_X(\omega) = E[|X(\omega)|^2]$ and $\phi_{V_1}(\omega) = E[|V_1(\omega)|^2]$ are the variances of $X(\omega)$ and $V_1(\omega)$, respectively, with $E[\cdot]$

denoting mathematical expectation. The output signal-to-noise ratio (oSNR) is defined as

$$\begin{aligned}\text{oSNR}[\mathbf{h}(\omega)] &= \phi_X(\omega)\frac{|\mathbf{h}^H(\omega)\mathbf{d}(\omega,1)|^2}{\mathbf{h}^H(\omega)\mathbf{\Phi}_{\mathbf{v}}(\omega)\mathbf{h}(\omega)}\\ &= \frac{\phi_X(\omega)}{\phi_{V_1}(\omega)}\times\frac{|\mathbf{h}^H(\omega)\mathbf{d}(\omega,1)|^2}{\mathbf{h}^H(\omega)\mathbf{\Gamma}_{\mathbf{v}}(\omega)\mathbf{h}(\omega)},\end{aligned} \tag{8}$$

where $\mathbf{\Phi}_{\mathbf{v}}(\omega)=E[\mathbf{v}(\omega)\mathbf{v}^H(\omega)]$ and $\mathbf{\Gamma}_{\mathbf{v}}(\omega)=\mathbf{\Phi}_{\mathbf{v}}(\omega)/\phi_{V_1}(\omega)$ are the correlation and pseudo-coherence matrices of $\mathbf{v}(\omega)$, respectively. The definition of the gain in SNR is easily derived from the previous definitions, i.e.,

$$\begin{aligned}\mathcal{G}[\mathbf{h}(\omega)] &= \frac{\text{oSNR}[\mathbf{h}(\omega)]}{\text{iSNR}(\omega)}\\ &= \frac{|\mathbf{h}^H(\omega)\mathbf{d}(\omega,1)|^2}{\mathbf{h}^H(\omega)\mathbf{\Gamma}_{\mathbf{v}}(\omega)\mathbf{h}(\omega)}.\end{aligned} \tag{9}$$

The most convenient way to evaluate the sensitivity of the array to some of its imperfections is via the so-called WNG (Cox *et al.*, 1987; Yan and Ma, 2005; Mabande *et al.*, 2009), which is defined by taking $\mathbf{\Gamma}_{\mathbf{v}}(\omega)=\mathbf{I}_M$ in Eq. (9), where $\mathbf{I}_M$ is the $M\times M$ identity matrix, i.e.,

$$\mathcal{W}[\mathbf{h}(\omega)] = \frac{|\mathbf{h}^H(\omega)\mathbf{d}(\omega,1)|^2}{\mathbf{h}^H(\omega)\mathbf{h}(\omega)}. \tag{10}$$

It is easy to check that the conventional delay-and-sum (DS) beamformer (Benesty *et al.*, 2008)

$$\mathbf{h}_{\text{DS}}(\omega) = \frac{\mathbf{d}(\omega,1)}{M}, \tag{11}$$

maximizes the WNG, i.e.,

$$\mathcal{W}[\mathbf{h}_{\text{DS}}(\omega)] = \mathcal{W}_{\max} = M. \tag{12}$$

Another important measure is the DF. Considering the spherically isotropic noise (sometime also called diffuse noise, meaning that the noise has an energy of equal probability from all directions) field, the DF is defined as

$$\mathcal{D}[\mathbf{h}(\omega)] = \frac{|\mathbf{h}^H(\omega)\mathbf{d}(\omega,1)|^2}{\mathbf{h}^H(\omega)\mathbf{\Gamma}_{\text{d}}(\omega)\mathbf{h}(\omega)}, \tag{13}$$

where the elements of the $M\times M$ matrix $\mathbf{\Gamma}_{\text{d}}(\omega)$ are

$$\begin{aligned}[\mathbf{\Gamma}_{\text{d}}(\omega)]_{i,j} &= \frac{\sin[\omega(j-i)\tau_0]}{\omega(j-i)\tau_0}\\ &= \text{sinc}[\omega(j-i)\tau_0],\end{aligned} \tag{14}$$

with $[\mathbf{\Gamma}_{\text{d}}(\omega)]_{m,m}=1$, $m=1,2,\ldots,M$. It can be checked that the superdirective beamformer (Cox *et al.*, 1986; Cox *et al.*, 1987),

$$\mathbf{h}_{\text{SD}}(\omega) = \frac{\mathbf{\Gamma}_{\text{d}}^{-1}(\omega)\mathbf{d}(\omega,1)}{\mathbf{d}^H(\omega,1)\mathbf{\Gamma}_{\text{d}}^{-1}(\omega)\mathbf{d}(\omega,1)}, \tag{15}$$

maximizes the DF, i.e.,

$$\mathcal{D}[\mathbf{h}_{\text{SD}}(\omega)] = \mathcal{D}_{\max}(\omega) = \mathbf{d}^H(\omega,1)\mathbf{\Gamma}_{\text{d}}^{-1}(\omega)\mathbf{d}(\omega,1). \tag{16}$$

Because it maximizes the DF, the superdirective beamformer is often called the supergain beamformer in the literature. It can be shown that (Uzkov, 1946)

$$\lim_{\delta\to 0}\mathcal{D}_{\max}(\omega) = M^2. \tag{17}$$

III. BEAMPATTERNS

The beampattern or directivity pattern describes the sensitivity of the beamformer to a plane wave (source signal) impinging on the array from the direction θ. For a uniform linear array, it is mathematically defined as

$$\begin{aligned}\mathcal{B}[\mathbf{h}(\omega),\cos\theta] &= \mathbf{d}^H(\omega,\cos\theta)\mathbf{h}(\omega)\\ &= \sum_{m=1}^{M}H_m(\omega)e^{\text{i}(m-1)\omega\tau_0\cos\theta}\\ &= \sum_{m=1}^{M}H_m(\omega)e^{\varpi_m\cos\theta},\end{aligned} \tag{18}$$

where $\varpi_m=\text{i}(m-1)\omega\tau_0$.

This paper is concerned with differential beamforming with DMAs, which is able to achieve frequency-invariant beampatterns. If omnidirectional sensors are used, the frequency-invariant beampattern of an Nth-order DMA can be expressed as (Elko, 2000; Benesty and Chen, 2012)

$$\mathcal{B}_N(\cos\theta) = \sum_{n=0}^{N}\alpha_n\cos^n\theta, \tag{19}$$

where $\theta\in[0,\pi]$ and α_n, $n=0,1,\ldots,N$ are real coefficients. The different values of these coefficients determine the different beampatterns of the Nth-order DMA. Assuming that $\alpha_N\neq 0$, $\mathcal{B}_N(\cos\theta)$ can be expressed as an algebraic polynomial of order N by taking $x=\cos\theta$, we get

$$\mathcal{B}_N(x) = \sum_{n=0}^{N}\alpha_n x^n, \tag{20}$$

where $x\in[-1,1]$. There are other ways to express Eq. (19) or, equivalently Eq. (20), as suggested in Abhayapala and Gupta (2010). In what follows, we derive a general form that is based on orthogonal polynomials.

Let $\mathcal{P}_n(x)$ be a polynomial of degree n, i.e., $\deg[\mathcal{P}_n(x)]=n$. A sequence of polynomials $\{\mathcal{P}_n(x)\}_{n=0}^{\infty}$ with $\deg[\mathcal{P}_n(x)]=n$ for each n is called orthogonal with respect to the weight function $w(x)$ on the interval $[-1,1]$ if (Chihara, 2011)

$$\int_{-1}^{1}w(x)\mathcal{P}_m(x)\mathcal{P}_n(x)dx = P_n\delta_{m,n}, \tag{21}$$

where $P_n\neq 0$ is a constant and

$$\delta_{m,n} = \begin{cases}0, & m\neq n\\ 1, & m=n.\end{cases} \tag{22}$$

The weight function, $w(x)$, should be defined on the interval $[-1,1]$ with $w(x)>0\,\forall x\in[-1,1]$, so that

$$\int_{-1}^{1} w(x)dx > 0. \tag{23}$$

The orthogonal polynomials $\{\mathcal{P}_0(x), \mathcal{P}_1(x), \ldots, \mathcal{P}_N(x)\}$ are linearly independent and, thus, form a basis for all polynomials of degree N. Therefore, every polynomial of degree N can be uniquely expressed as a linear combination of the orthogonal polynomials (Chihara, 2011). So, we can rewrite Eq. (20) as

$$\mathcal{B}_N(x) = \sum_{n=0}^{N} \beta_n \mathcal{P}_n(x), \tag{24}$$

where

$$\beta_n = \frac{\int_{-1}^{1} w(x)\mathcal{B}_N(x)\mathcal{P}_n(x)dx}{\int_{-1}^{1} w(x)\mathcal{P}_n^2(x)dx}, \quad n = 0, 1, \ldots, N. \tag{25}$$

Let $f(x)$ be a continuous function in $[-1, 1]$. Its series expansion in terms of $\{\mathcal{P}_n(x)\}_{n=0}^{\infty}$ is

$$f(x) = \sum_{n=0}^{\infty} a_n \mathcal{P}_n(x), \tag{26}$$

where

$$a_n = \frac{\int_{-1}^{1} w(x)f(x)\mathcal{P}_n(x)dx}{\int_{-1}^{1} w(x)\mathcal{P}_n^2(x)dx}, \quad n = 0, 1, 2, \ldots. \tag{27}$$

In particular, we have

$$e^{\varpi_m x} = \sum_{n=0}^{\infty} b_n(\varpi_m)\mathcal{P}_n(x), \tag{28}$$

where

$$b_n(\varpi_m) = \frac{\int_{-1}^{1} w(x)e^{\varpi_m x}\mathcal{P}_n(x)dx}{\int_{-1}^{1} w(x)\mathcal{P}_n^2(x)dx}, \quad n = 0, 1, 2, \ldots. \tag{29}$$

Substituting Eq. (28) into Eq. (18), we get

$$\begin{aligned}
\mathcal{B}[\mathbf{h}(\omega), x] &= \sum_{m=1}^{M} H_m(\omega)e^{\varpi_m x} \\
&= \sum_{m=1}^{M} H_m(\omega) \sum_{n=0}^{\infty} b_n(\varpi_m)\mathcal{P}_n(x) \\
&= \sum_{n=0}^{\infty} \mathcal{P}_n(x) \left[\sum_{m=1}^{M} b_n(\varpi_m)H_m(\omega)\right] \\
&= \sum_{n=0}^{\infty} \mathcal{P}_n(x)\mathbf{b}_n^T(\omega)\mathbf{h}(\omega),
\end{aligned} \tag{30}$$

where

$$\mathbf{b}_n(\omega) = [\, b_n(\varpi_1) \quad b_n(\varpi_2) \quad \cdots \quad b_n(\varpi_M) \,]^T. \tag{31}$$

If we limit the expansion to the order N, $\mathcal{B}[\mathbf{h}(\omega), x]$ can be approximated by

$$\mathcal{B}_N[\mathbf{h}(\omega), x] = \sum_{n=0}^{N} \mathcal{P}_n(x)\mathbf{b}_n^T(\omega)\mathbf{h}(\omega). \tag{32}$$

In Sec. IV, we will see how to design DMAs of any order using the previous expression.

IV. DMA DESIGN

In this section, we discuss how to design frequency-invariant beampatterns with DMAs. We divide the general design issue into two cases. The first case is concerned with the scenario where the number of microphones in the DMA is equal to the order of the DMA plus 1. The resulting beamformers are called non-robust ones as they may greatly suffer from white noise amplification, particularly at low frequencies. The second case discusses the situation where the number of microphones in the DMA is greater than the order of the DMA plus 1. The resulting beamformers are called robust beamformers as they have less white noise amplification as compared to those in the first category.

A. Non-robust

In the non-robust case, we have $M = N + 1$, which is the condition that all the conventional DMAs are used. We would like to find the filter $\mathbf{h}(\omega)$ in such a way that $\mathcal{B}_{M-1}[\mathbf{h}(\omega), x]$ is an Nth-order frequency-invariant beampattern, i.e.,

$$\mathcal{B}_{M-1}[\mathbf{h}(\omega), x] = \mathcal{B}_{M-1}(x). \tag{33}$$

By simple identification between Eqs. (32) and (24), we easily find that

$$\mathbf{B}(\omega)\mathbf{h}(\omega) = \boldsymbol{\beta}, \tag{34}$$

where

$$\mathbf{B}(\omega) = \begin{bmatrix} \mathbf{b}_0^T(\omega) \\ \mathbf{b}_1^T(\omega) \\ \vdots \\ \mathbf{b}_{M-1}^T(\omega) \end{bmatrix} \tag{35}$$

is an $M \times M$ matrix, and

$$\boldsymbol{\beta} = [\, \beta_0 \quad \beta_1 \quad \cdots \quad \beta_{M-1} \,]^T \tag{36}$$

is a vector of length M containing the coefficients of the Nth-order frequency-invariant DMA beampattern. Assuming that $\mathbf{B}(\omega)$ is a full-rank matrix, we find that the non-robust filter is

$$\mathbf{h}_{\mathrm{NR}}(\omega) = \mathbf{B}^{-1}(\omega)\boldsymbol{\beta}, \tag{37}$$

where the subscript NR stands for "non-robust."

Ideally, we would like to find the orthogonal polynomials $\{\mathcal{P}_0(x), \mathcal{P}_1(x), \ldots, \mathcal{P}_{M-1}(x)\}$ that can give a good compromise between WNG and DF.

B. Robust

In the robust scenario, the number of microphones is greater than the DMA order plus 1, i.e., $M > N+1$. Again, we would like to find the filter $\mathbf{h}(\omega)$ in such a way that $\mathcal{B}_N[\mathbf{h}(\omega), x]$ is an Nth-order frequency-invariant beampattern, i.e.,

$$\mathcal{B}_N[\mathbf{h}(\omega), x] = \mathcal{B}_N(x). \tag{38}$$

By simple identification, we easily find that

$$\mathbf{B}'(\omega)\mathbf{h}(\omega) = \boldsymbol{\beta}, \tag{39}$$

where

$$\mathbf{B}'(\omega) = \begin{bmatrix} \mathbf{b}_0^T(\omega) \\ \mathbf{b}_1^T(\omega) \\ \vdots \\ \mathbf{b}_N^T(\omega) \end{bmatrix} \tag{40}$$

is now an $(N+1)\times M$ matrix. Assuming that $\mathbf{B}'^H(\omega)$ is a full column rank matrix and taking the minimum-norm solution of Eq. (39), we find that the robust filter is

$$\mathbf{h}_{\mathrm{R}}(\omega) = \mathbf{B}'^H(\omega)[\mathbf{B}'(\omega)\mathbf{B}'^H(\omega)]^{-1}\boldsymbol{\beta}, \tag{41}$$

where the subscript $_{\mathrm{R}}$ stands for "robust."

The choice of the orthogonal polynomials is important in practice in order to better design a desired beampattern.

C. Constant beampattern

In this subsection, we discuss how to design beamformers with a frequency-invariant beampattern or constant beampattern for short.

We define the square norm of $\mathcal{B}[\mathbf{h}(\omega), x]$ with respect to the weight function $w(x)$ as

$$\begin{aligned} \|\mathcal{B}[\mathbf{h}(\omega), x]\|_w^2 &= \frac{1}{P_0}\int_{-1}^{1} w(x)|\mathcal{B}[\mathbf{h}(\omega), x]|^2 dx \\ &= \mathbf{h}^H(\omega)\boldsymbol{\Gamma}_w(\omega)\mathbf{h}(\omega), \end{aligned} \tag{42}$$

where

$$\boldsymbol{\Gamma}_w(\omega) = \frac{1}{P_0}\int_{-1}^{1} w(x)\mathbf{d}(\omega, x)\mathbf{d}^H(\omega, x)dx. \tag{43}$$

To design a constant beampattern, we can minimize $\|\mathcal{B}[\mathbf{h}(\omega), x]\|_w^2$ subject to Eq. (39), i.e.,

$$\min_{\mathbf{h}(\omega)} \mathbf{h}^H(\omega)\boldsymbol{\Gamma}_w(\omega)\mathbf{h}(\omega) \ \text{ subject to } \ \mathbf{B}'(\omega)\mathbf{h}(\omega) = \boldsymbol{\beta}, \tag{44}$$

which actually minimizes the beampattern error in the weighted least-squares (WLS) sense; see the proof in Appendix A. We easily find that the solution is

$$\begin{aligned} \mathbf{h}_{\mathrm{CP}}(\omega) = &\boldsymbol{\Gamma}_w^{-1}(\omega)\mathbf{B}'^H(\omega) \\ &\times [\mathbf{B}'(\omega)\boldsymbol{\Gamma}_w^{-1}(\omega)\mathbf{B}'^H(\omega)]^{-1}\boldsymbol{\beta}, \end{aligned} \tag{45}$$

where the subscript CP stands for "constant beampattern."

To better compromise with white noise amplification, we can use the following regularized CP beamformer

$$\begin{aligned} \mathbf{h}_{\mathrm{CP},\epsilon}(\omega) = &\boldsymbol{\Gamma}_{w,\epsilon}^{-1}(\omega)\mathbf{B}'^H(\omega) \\ &\times [\mathbf{B}'(\omega)\boldsymbol{\Gamma}_{w,\epsilon}^{-1}(\omega)\mathbf{B}'^H(\omega)]^{-1}\boldsymbol{\beta}, \end{aligned} \tag{46}$$

where

$$\boldsymbol{\Gamma}_{w,\epsilon}(\omega) = \boldsymbol{\Gamma}_w(\omega) + \epsilon\mathbf{I}_M, \tag{47}$$

with $\epsilon \geq 0$ being the regularization parameter. It is clear that $\mathbf{h}_{\mathrm{CP},0}(\omega) = \mathbf{h}_{\mathrm{CP}}(\omega)$. Now, if we rearrange $\boldsymbol{\Gamma}_{w,\epsilon}(\omega)$ as $\boldsymbol{\Gamma}_{w,\epsilon}(\omega) = \epsilon[(1/\epsilon)\boldsymbol{\Gamma}_w(\omega) + \mathbf{I}_M]$ and then substitute this into Eq. (46), we can find that $\mathbf{h}_{\mathrm{CP},\infty}(\omega) = \mathbf{h}_{\mathrm{R}}(\omega)$.

V. JACOBI POLYNOMIALS

The Jacobi polynomials (Chihara, 2011), $\mathcal{P}_n^{(\imath,\jmath)}(x)$, are a class of classical orthogonal polynomials that are orthogonal with respect to the weight function $w^{(\imath,\jmath)}(x) = (1-x)^{\imath}(1+x)^{\jmath}$ on the interval $[-1, 1]$, i.e.,

$$\int_{-1}^{1} w^{(\imath,\jmath)}(x)\mathcal{P}_m^{(\imath,\jmath)}(x)\mathcal{P}_n^{(\imath,\jmath)}(x)dx = P_n\delta_{m,n}, \tag{48}$$

where

$$P_n = \frac{2^{\imath+\jmath+1}}{2n+\imath+\jmath+1} \times \frac{\Gamma(n+\imath+1)\Gamma(n+\jmath+1)}{n!\Gamma(n+\imath+\jmath+1)}, \tag{49}$$

with $\Gamma(\cdot)$ being the Gamma function. The parameters $\imath$ and $\jmath$ are real numbers, which are restricted to $\imath, \jmath > -1$, for integrability purposes. Many well known orthogonal polynomials such as Legendre, Chebyshev, and Gegenbauer can be viewed as particular cases of the Jacobi polynomials; this is what makes the Jacobi polynomials so much interesting. They are defined by the Rodrigues type formula,

$$\begin{aligned} \mathcal{P}_n^{(\imath,\jmath)}(x) = &\frac{(-1)^n}{2^n n!}(1-x)^{-\imath}(1+x)^{-\jmath} \\ &\times \frac{d^n}{dx^n}\left[(1-x)^{\imath}(1+x)^{\jmath}(1-x^2)^n\right]. \end{aligned} \tag{50}$$

The Jacobi polynomials can be conveniently generated by the three-term recurrence relation

$$\mathcal{P}_{n+1}^{(\imath,\jmath)}(x)=(a_n^{(\imath,\jmath)}x-b_n^{(\imath,\jmath)})\mathcal{P}_n^{(\imath,\jmath)}(x)-c_n^{(\imath,\jmath)}\mathcal{P}_{n-1}^{(\imath,\jmath)}(x),\quad n\geq 1, \tag{51}$$

where

$$a_n^{(\imath,\jmath)}=\frac{(2n+\imath+\jmath+1)(2n+\imath+\jmath+2)}{2(n+1)(n+\imath+\jmath+1)}, \tag{52}$$

$$b_n^{(\imath,\jmath)}=\frac{(\jmath^2-\imath^2)(2n+\imath+\jmath+1)}{2(n+1)(n+\imath+\jmath+1)(2n+\imath+\jmath)}, \tag{53}$$

$$c_n^{(\imath,\jmath)}=\frac{(n+\imath)(n+\jmath)(2n+\imath+\jmath+2)}{(n+1)(n+\imath+\jmath+1)(2n+\imath+\jmath)}, \tag{54}$$

with

$$\mathcal{P}_0^{(\imath,\jmath)}(x)=1, \tag{55}$$

$$\mathcal{P}_1^{(\imath,\jmath)}(x)=\frac{1}{2}(\imath+\jmath+2)x+\frac{1}{2}(\imath-\jmath). \tag{56}$$

In practice, the coefficients α_n, $n=0,1,\ldots,N$ in the definition of the DMA beampattern in Eq. (20) are well known for all desired beampatterns. Because the coefficients β_n, $n=0,1,\ldots,N$ are involved in the design of the DMA beampatterns, as it can be observed in Eqs. (37), (41), (45), and (46), it is important to determine them as a function of the α_n's. By simple identification between Eqs. (20) and (24) and using the Jacobi polynomials, $\mathcal{P}_n^{(\imath,\imath)}(x)$, we show how to compute the β_n's in Appendix B.

VI. NUMERICAL STUDY

In this section, we provide some examples to illustrate how to design frequency-invariant beampatterns with DMAs. In particular, we consider the design of the

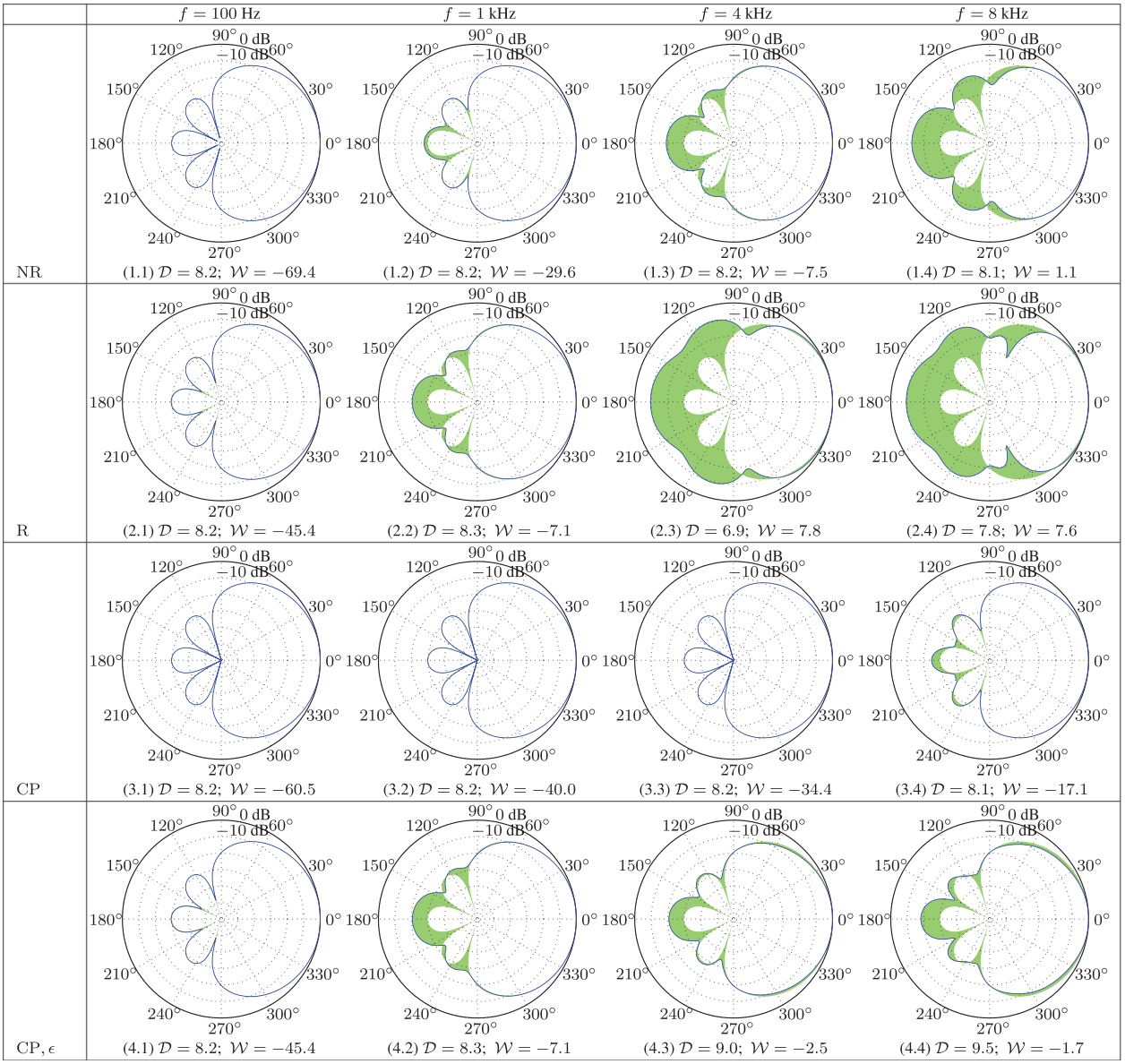

FIG. 1. Beampatterns of the non-robust (NR), robust (R), CP, and regularized CP (CP, ϵ) filters, where $M=3$ for the NR filter, $M=8$ for the others, $\delta=1$ cm, $\epsilon=10^{-3}$ for the regularized CP filter, and $(\imath,\jmath)=(0,0)$. The desired beampattern is the second-order supercardioid. The green area shows the difference between the desired and designed beampatterns.

supercardioid of different orders. The frequency-invariant first-, second-, and third-order supercardioid beampatterns are given by (De Sena *et al.*, 2012)

$$\mathcal{B}_{1,\mathrm{SC}}(x) = 0.414 + 0.586x, \tag{57}$$

$$\mathcal{B}_{2,\mathrm{SC}}(x) = 0.103 + 0.484x + 0.413x^2, \tag{58}$$

$$\mathcal{B}_{3,\mathrm{SC}}(x) = 0.022 + 0.217x + 0.475x^2 + 0.286x^3, \tag{59}$$

where $x = \cos\theta$. The design is made with the different filters proposed in Sec. IV and the Jacobi polynomials with different values of the pair $(\imath, \jmath)$ as shown in Sec. V.

A. Influence of the filters

In this subsection, we design the second-order supercardioid with the non-robust, robust, CP, and regularized CP filters to evaluate their performance. The beampatterns and SNR gains are plotted in Figs. 1 and 2, respectively, where $N = 2$, $M = 3$ for the non-robust filter, $M = 8$ for the others, $\delta = 1$ cm, $\epsilon = 10^{-3}$ for the regularized CP filter, $(\imath, \jmath) = (0, 0)$, and the difference between the desired and designed beampatterns is marked in green.

The beampatterns obtained with the non-robust filter are almost frequency invariant as long as $\omega\tau_0 \ll 2\pi$, as shown in Figs. 1(1.1) and 1(1.2) [where (1.1) is the subplot in the first row and first column and (1.2) is the subplot in the first row and second column; in what follows, $(l.k)$ denotes the subplot in the lth row and kth column of the figure]; however, the beampattern diverges as the frequency increases when this assumption does not hold [see Figs. 1(1.3) and 1(1.4)]. It is interesting to observe that the DF of this beamformer is almost constant although the beampatterns at high frequencies are different from those at low frequencies [see the dash black line in Fig. 2(a)]. The underlying reason is that the mainlobe gets slightly narrower while the sidelobes get larger [see Fig. 1(1.4)]. It is clearly seen from Fig. 2(b) (the dash black line) that the non-robust filter suffers from white noise amplification and the amount of white noise amplification increases as the frequency decreases.

The robust beamformer greatly improves the WNG [see the dash-dot blue line in Fig. 2(b)]; especially at low frequencies where the improvement is more than 20 dB as compared to the non-robust case. Note that the robust beamformer uses more sensors, and therefore the array is larger in aperture as compared to that with the non-robust method. The beampattern with the robust beamformer changes as the frequency increases [see Figs. 1(2.2), 1(2.3), and 1(2.4)], which also causes the degradation of the corresponding DF [see the dash-dot black line in Fig. 2(a)].

The beampattern of the CP filter is almost frequency invariant [see Figs. 1(3.1), 1(3.2), 1(3.3), and 1(3.4)], so is the DF [see the dotted green line in Fig. 2(a)]. However, this beamformer dramatically suffers from the white noise amplification problem [see the dot green line in Fig. 2(b)]; it is even worse than the non-robust filter.

The beampatterns of the regularized CP filter are plotted in Figs. 1(4.1), 1(4.2), 1(4.3), and 1(4.4). One can see that the designed beampatterns resemble the desired beampattern at low frequencies; interestingly, the mainlobe gets narrower and narrower as the frequency increases, which causes the DF to increase with frequency [see the solid red line in Fig. 2(a)]. The WNG of the regularized CP filter is almost the same as the one obtained with the robust filter at low frequencies [see the solid red line in Fig. 2(b)]. Consequently we can state that this beamformer can be very useful in practice.

B. Influence of the Jacobi parameters

Among the four proposed filters, the regularized CP filter seems to be the most interesting one. In this subsection, we show how the regularized CP filter works for different values of the pair $(\imath, \jmath)$. To fairly compare the performance of this beamformer for different conditions of the Jacobi parameters, we choose the values of the regularization parameter that give the same WNG. Figure 3 plots the beampatterns of the regularized CP filter for different values of the pair $(\imath, \jmath)$, where the WNG is 0 dB at 4 kHz, $M = 8$, and $\delta = 1$ cm. The corresponding values of the regularization parameter are shown in Table I. It can be seen that the beampatterns diverge more or less from the desired one in different ways.

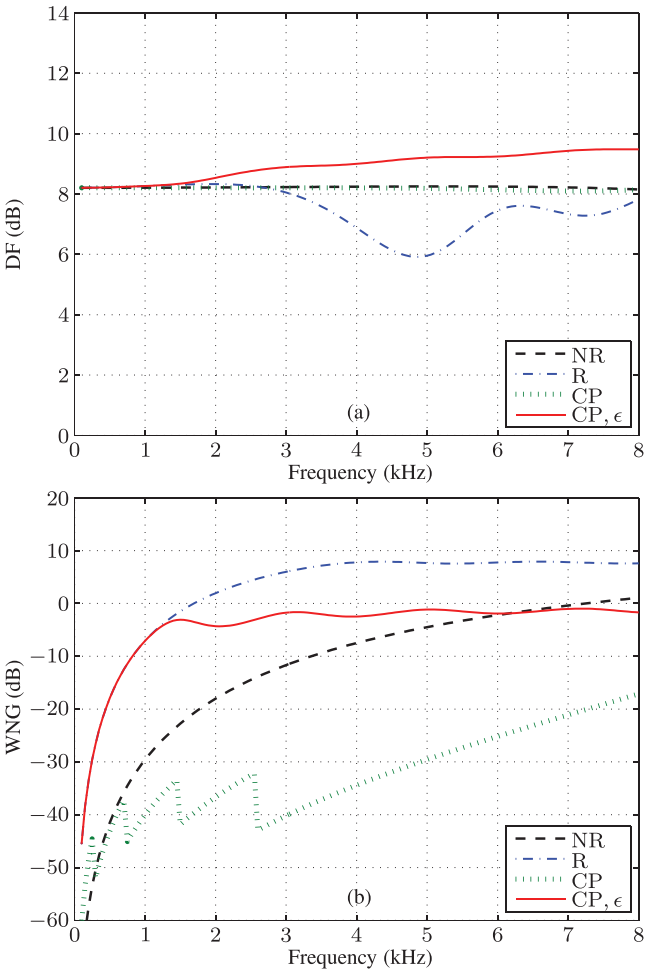

FIG. 2. SNR gains of the NR, R, CP, and CP, ϵ filters, where $M = 3$ for the NR filter, $M = 8$ for the others, $\delta = 1$ cm, $\epsilon = 10^{-3}$ for the regularized CP filter, and $(\imath, \jmath) = (0, 0)$. The desired beampattern is the second-order supercardioid.

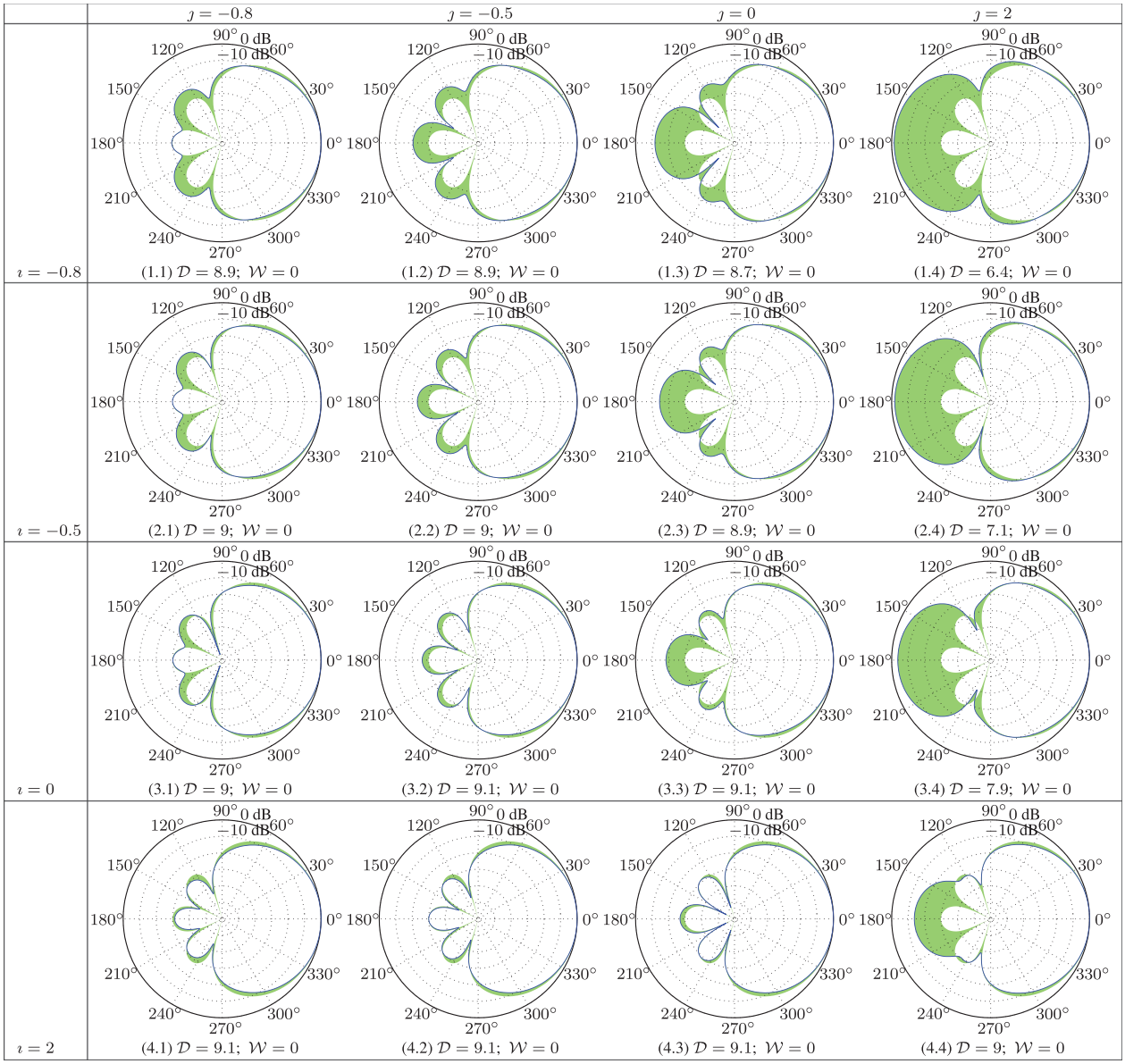

FIG. 3. Beampatterns of the regularized CP filter for different values of the pair $(\imath, \jmath)$. The WNG is 0 dB, $M = 8$, $\delta = 1$ cm, and $f = 4$ kHz. The desired beampattern is the second-order supercardioid. The green area shows the difference between the desired and designed beampatterns.

To investigate the behavior of these beampatterns and get further insight into the choice of the pair $(\imath, \jmath)$, we can rewrite the optimization problem of the regularized CP filter as

$$\min_{\mathbf{h}(\omega)} \frac{1}{P_0}\int_0^{\pi} \psi^{(\imath,\jmath)}(\theta)|\varepsilon[\mathbf{h}(\omega), \cos\theta]|^2 d\theta \quad \text{subject to } \mathbf{h}^H(\omega)\mathbf{h}(\omega) = \gamma,\ \mathbf{B}'(\omega)\mathbf{h}(\omega) = \boldsymbol{\beta}, \tag{60}$$

TABLE I. Values of the regularization parameter in the regularized CP filter for different values of the pair $(\imath, \jmath)$. The WNG is 0 dB at $f = 4$ kHz, $M = 8$, and $\delta = 1$ cm.

Regularization parameter ϵ ($\times 10^{-5}$)				
	$\jmath = -0.8$	$\jmath = -0.5$	$\jmath = 0$	$\jmath = 2$
$\imath = -0.8$	345.99	410.47	378.55	582.94
$\imath = -0.5$	262.98	403.15	429.35	736.53
$\imath = 0$	119.71	222.67	286.44	352.27
$\imath = 2$	6.79	17.62	33.68	55.73

where $\varepsilon[\mathbf{h}(\omega), \cos\theta]$ is defined in Appendix A,

$$\psi^{(\imath,\jmath)}(\theta) = w^{(\imath,\jmath)}(\cos\theta)\sin\theta = (1-\cos\theta)^{\imath}(1+\cos\theta)^{\jmath}\sin\theta \tag{61}$$

is the weight function with respect to θ, and γ is determined by the minimum WNG. This weight function determines the error distribution in the optimization process. As we will see, by properly setting this function, we can improve the performance of the DMA beampattern design. We propose to divide the weight function into the following four cases:

(1) $\imath > \jmath, \jmath \le -0.5$. In this case, the weight function can be written as

$$\psi^{(\imath,\jmath)}(\theta) = (1-\cos\theta)^{\imath-\jmath}\sin^{2\jmath+1}\theta. \tag{62}$$

As $\imath$ increases, the beampattern error in the backward-side becomes smaller and smaller, as shown in

TABLE II. Values of the regularization parameter in the regularized CP filter for different weight functions. The WNG is -5 dB at $f=4$ kHz, $M=8$, and $\delta=1$ cm.

	$(\iota,\jmath)$	ϵ
BC (backward-facing-cardioid)	(2,−0.5)	9.5×10^{-6}
FC (forward-facing-cardioid)	(−0.5,1)	1.9×10^{-3}
D (dipole)	(−0.8,−0.8)	5×10^{-4}
O (omnidirectional)	(−0.5,−0.5)	6×10^{-4}

Figs. 3(2.1), 3(3.1), and 3(4.1) [see also Fig. 3(3.2) and 3(4.2)]. A typical weight function for this case is

$$\psi_{\mathrm{BC}}^{(\iota,-0.5)}(\theta)=(1-\cos\theta)^{\iota+0.5},\ \iota>-0.5, \tag{63}$$

which is the backward-facing-cardioid-like beampattern, where the subscript $_{\mathrm{BC}}$ stands for backward facing cardioid.

(2) $\jmath>\iota,\iota\le-0.5$. In this case, the weight function can be expressed as

$$\psi^{(\iota,\jmath)}(\theta)=(1+\cos\theta)^{\jmath-\iota}\sin^{2\iota+1}\theta. \tag{64}$$

As ι increases, the sidelobe should be larger and larger, as shown in Figs. 3(1.2), 3(1.3), and 3(1.4) [see also Figs. 3(2.3) and 3(2.4)]. A typical particular case is

$$\psi_{\mathrm{FC}}^{(-0.5,\jmath)}(\theta)=(1+\cos\theta)^{\jmath+0.5},\jmath>-0.5, \tag{65}$$

which is the forward-facing-cardioid-like beampattern, where the subscript FC stands for forward facing cardioid.

(3) $\iota=\jmath=-0.5$. In this case, the weight function is

$$\psi_{\mathrm{O}}^{(\iota,\jmath)}(\theta)=1, \tag{66}$$

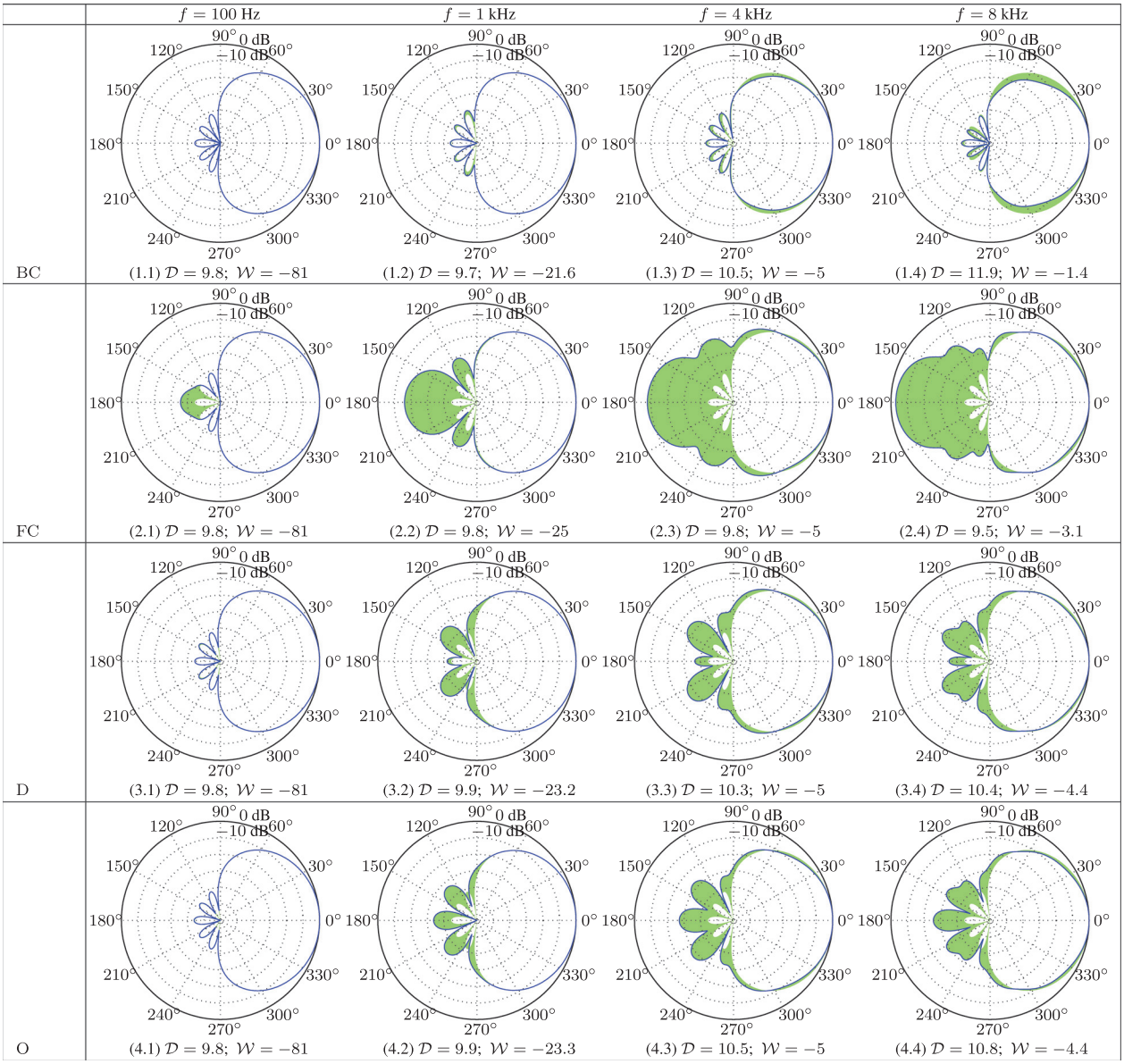

FIG. 4. Beampatterns of the regularized CP filter for different weight functions where $M=8$ and $\delta=1$ cm. The desired beampattern is the third-order supercardioid. The green area shows the difference between the desired and designed beampatterns.

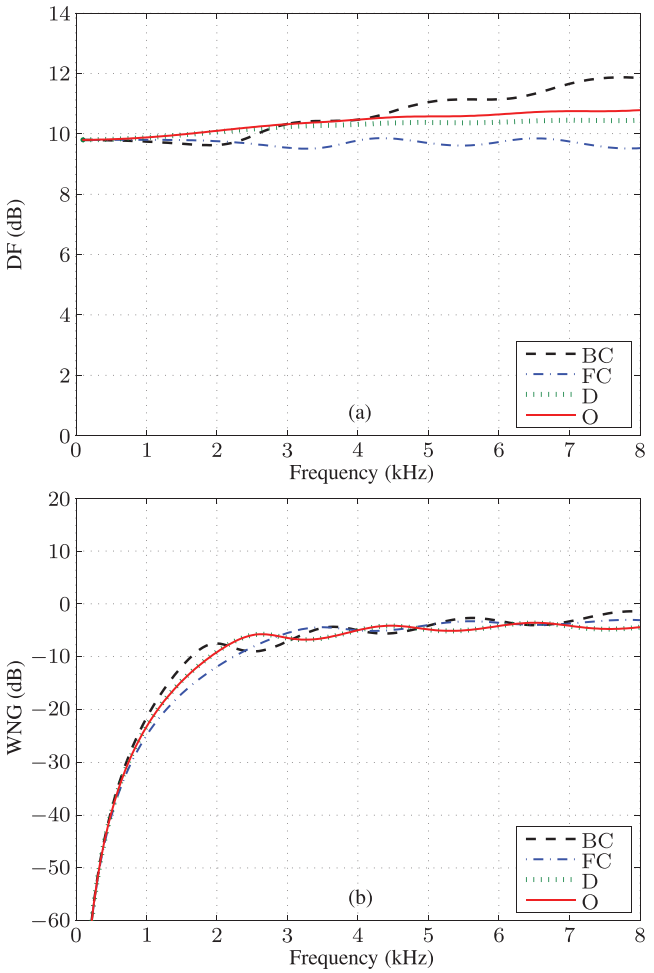

FIG. 5. SNR gains of the regularized CP filter for different weight functions where $M=8$ and $\delta=1$ cm. The desired beampattern is the third-order supercardioid.

which is the omnidirectional beampattern, where the subscript $_{\mathrm{O}}$ stands for omnidirectional. An example is given in Fig. 3(2.2).

(4) $-1<\imath=\jmath<-0.5$. In this case, the weight function is

$$\psi_{\mathrm{D}}^{(\imath,\jmath)}(\theta)=\sin^{2\imath+1}\theta, \tag{67}$$

which is the dipole-like beampattern, the subscript D stands for dipole. An example is shown in Fig. 3(1.1).

Now, we evaluate the performance of the regularized CP filter with $M=8$ and $\delta=1$ cm for the design of the third-order supercardioid with the above four choices of the weight function. The values of the regularization parameter for a -5 dB WNG at 4 kHz are shown in Table II for typical values of the pair $(\imath,\jmath)$. The beampatterns and SNR gains corresponding to the regularized CP filter for different cases of the weight function are shown in Figs. 4 and 5, respectively. The behavior of the beampatterns coincide with the previous analysis very well and the SNR gains for the different values of $(\imath,\jmath)$ are very close to each other.

VII. CONCLUSIONS

In this paper, we proposed a general and flexible approach to the design of DMAs. First, we showed how to express the beampatterns as a function of orthogonal polynomials, from which we deduced a good approximation of any beamformer beampattern. With this approximation, we then developed four differential beamformers, namely, non-robust, robust, CP, and regularized CP. Of particular importance is the regularized CP beamformer, which can greatly improve the WNG at low frequencies and meanwhile makes the designed beampatten closer to the desired one at high frequencies. Finally, we showed how to use the Jacobi polynomials in this context with which, by choosing proper parameters, we can design all kinds of DMA beampatterns of any orders and also control the matching between the designed beampattern and the desired one.

ACKNOWLEDGMENT

This work was supported in part by the NSFC "Distinguished Young Scientists Fund" under Grant No. 61425005. Research by the first author is also supported in part by China Scholarship Council.

APPENDIX A: EQUIVALENT FORM OF EQ. (44)

Using the constraint Eq. (39) in Eq. (30), we get

$$\mathcal{B}[\mathbf{h}(\omega),x]=\sum_{n=0}^{N}\beta_n\mathcal{P}_n(x)+\varepsilon[\mathbf{h}(\omega),x], \tag{A1}$$

where

$$\varepsilon[\mathbf{h}(\omega),x]=\sum_{n=N+1}^{\infty}\mathcal{P}_n(x)\mathbf{b}_n^T(\omega)\mathbf{h}(\omega) \tag{A2}$$

is the error between the designed and desired beampatterns.

Substituting Eq. (A1) into Eq. (42), and taking Eq. (21) into account, we can rewrite the cost function as

$$\|\mathcal{B}[\mathbf{h}(\omega),x]\|_w^2=\sum_{n=0}^{N}\frac{P_n}{P_0}\beta_n^2+\mathrm{WLS}[\mathbf{h}(\omega)], \tag{A3}$$

where

$$\mathrm{WLS}[\mathbf{h}(\omega)]=\frac{1}{P_0}\int_{-1}^{1}w(x)|\varepsilon[\mathbf{h}(\omega),x]|^2dx \tag{A4}$$

is the weighted least-squares (WLS) criterion. It follows immediately that Eq. (44) is equivalent to

$$\min_{\mathbf{h}(\omega)}\mathrm{WLS}[\mathbf{h}(\omega)]\ \text{ subject to }\ \mathbf{B}'(\omega)\mathbf{h}(\omega)=\boldsymbol{\beta}. \tag{A5}$$

APPENDIX B: RELATIONSHIP BETWEEN THE α_n's AND β_n's

Let us first express the nth-order orthogonal polynomial as

$$\mathcal{P}_n^{(\imath,\jmath)}(x)=\sum_{i=0}^{n}\xi_{n,i}x^i=\boldsymbol{\xi}_n^T\mathbf{x}_n, \tag{B1}$$

where

$$\boldsymbol{\xi}_n = [\,\xi_{n,0} \quad \xi_{n,1} \quad \cdots \quad \xi_{n,n}\,]^T, \tag{B2}$$

$$\mathbf{x}_n = [\,1 \quad x \quad \cdots \quad x^n\,]^T \tag{B3}$$

are vectors of length $n+1$. Using Eq. (B1), the recurrence relation in Eq. (51) can be expressed as

$$\begin{aligned}\mathcal{P}_{n+1}^{(\iota,\jmath)}(x) &= \boldsymbol{\xi}_{n+1}^T \mathbf{x}_{n+1} \\ &= (\mathbf{R}_n \boldsymbol{\xi}_n)^T \mathbf{x}_{n+1} - (\mathbf{R}_{n-1}\boldsymbol{\xi}_{n-1})^T \mathbf{x}_{n+1},\ n \geq 1,\end{aligned} \tag{B4}$$

where

$$\mathbf{R}_n = a_n^{(i,j)} \begin{bmatrix} 0_{1\times(n+1)} \\ \mathbf{I}_{(n+1)\times(n+1)} \end{bmatrix} - b_n^{(i,j)} \begin{bmatrix} \mathbf{I}_{(n+1)\times(n+1)} \\ 0_{1\times(n+1)} \end{bmatrix}, \tag{B5}$$

$$\mathbf{R}_{n-1} = c_n^{(i,j)} \begin{bmatrix} \mathbf{I}_{n\times n} \\ 0_{2\times n} \end{bmatrix}, \tag{B6}$$

with $\mathbf{I}_{K\times K}$ and $0_{K\times L}$ being the identity matrix of size $K\times K$ and the zero matrix of size $K\times L$, respectively.

From Eq. (B4), the coefficients of the orthogonal polynomial can be recursively computed as

$$\boldsymbol{\xi}_{n+1} = \mathbf{R}_n \boldsymbol{\xi}_n - \mathbf{R}_{n-1}\boldsymbol{\xi}_{n-1},\ n \geq 1, \tag{B7}$$

with

$$\boldsymbol{\xi}_0 = 1, \tag{B8}$$

$$\boldsymbol{\xi}_1 = \left[\frac{1}{2}(\iota - \jmath) \quad \frac{1}{2}(\iota + \jmath + 2)\right]^T. \tag{B9}$$

Substituting Eq. (B1) into Eq. (24), we can express the beampattern as

$$\begin{aligned}\mathcal{B}_N(x) &= \sum_{n=0}^{N} \beta_n \boldsymbol{\xi}_n^T \mathbf{x}_n \\ &= [\,\mathbf{x}_0^T\boldsymbol{\xi}_0 \quad \mathbf{x}_1^T\boldsymbol{\xi}_1 \quad \cdots \quad \mathbf{x}_N^T\boldsymbol{\xi}_N\,]\boldsymbol{\beta} \\ &= \mathbf{x}_N^T \boldsymbol{\Xi}_{\alpha,\beta}\boldsymbol{\beta},\end{aligned} \tag{B10}$$

where

$$\boldsymbol{\Xi}_{\alpha,\beta} = \begin{bmatrix} \xi_{0,0} & \xi_{1,0} & \xi_{2,0} & \cdots & \xi_{N,0} \\ 0 & \xi_{1,1} & \xi_{2,1} & \cdots & \xi_{N,1} \\ 0 & 0 & \xi_{2,2} & \cdots & \xi_{N,2} \\ \vdots & \vdots & \vdots & \ddots & \vdots \\ 0 & 0 & 0 & \cdots & \xi_{N,N} \end{bmatrix} \tag{B11}$$

is an upper-triangular matrix of size $(N+1)\times(N+1)$ and

$$\boldsymbol{\beta} = [\,\beta_0 \quad \beta_1 \quad \cdots \quad \beta_N\,]^T. \tag{B12}$$

Using Eq. (20) with Eq. (B10), we finally deduce the relationship between the coefficients α_n and β_n

$$\boldsymbol{\beta} = \boldsymbol{\Xi}_{\alpha,\beta}^{-1}\boldsymbol{\alpha}, \tag{B13}$$

where

$$\boldsymbol{\alpha} = [\,\alpha_0 \quad \alpha_1 \quad \cdots \quad \alpha_N\,]^T. \tag{B14}$$

Abhayapala, T. D., and Gupta, A. (**2010**). "Higher order differential-integral microphone arrays," J. Acoust. Soc. Am. **127**, EL227–EL233.

Benesty, J., and Chen, J. (**2012**). *Study and Design of Differential Microphone Arrays* (Springer-Verlag, Berlin, Germany).

Benesty, J., Chen, J., and Huang, Y. (**2008**). *Microphone Array Signal Processing* (Springer-Verlag, Berlin, Germany).

Benesty, J., Chen, J., Huang, Y., and Dmochowski, J. (**2007**). "On microphone-array beamforming from a MIMO acoustic signal processing perspective," IEEE Trans. Audio, Speech Lang. Process. **15**, 1053–1065.

Buck, M. (**2002**). "Aspects of first-order differential microphone arrays in the presence of sensor imperfections," Eur. Trans. Telecommun. **13**, 115–122.

Chen, J., Benesty, J., and Pan, C. (**2014**). "On the design and implementation of linear differential microphone arrays," J. Acoust. Soc. Am. **136**, 3097–3113.

Chihara, T. S. (**2011**). *An Introduction to Orthogonal Polynomials* (Dover, New York).

Chou, T. (**1995**). "Frequency-independent beamformer with low response error," in *Proceedings of the IEEE International Conference on Acoustics, Speech, and Signal Processing (ICASSP)*, Vol. 5, pp. 2995–2998.

Cox, H., Zeskind, R. M., and Kooij, T. (**1986**). "Practical supergain," IEEE Trans. Acoust. Speech Signal Process. **34**, 393–398.

Cox, H., Zeskind, R. M., and Owen, M. M. (**1987**). "Robust adaptive beamforming," IEEE Trans. Acoust. Speech Signal Process. **35**, 1365–1376.

De Sena, E., Hacihabiboglu, H., and Cvetkovic, Z. (**2012**). "On the design and implementation of higher-order differential microphones," IEEE Trans. Audio Speech Lang. Process. **20**, 162–174.

Doclo, S., and Moonen, M. (**2003**). "Design of broadband beamformers robust against gain and phase errors in the microphone array characteristics," IEEE Trans. Signal Process. **51**, 2511–2526.

Elko, G. W. (**2000**). "Superdirectional microphone arrays," in *Acoustic Signal Processing for Telecommunication*, edited by S. L. Gay and J. Benesty (Kluwer Academic, Boston, MA), Chap. 10, pp. 181–237.

Elko, G. W., and Meyer, J. (**2008**). "Microphone arrays," in *Springer Handbook of Speech Processing*, edited by J. Benesty, M. M. Sondhi, and Y. Huang (Springer-Verlag, Berlin, Germany), Chap. 50, pp. 1021–1041.

Mabande, E., Schad, A., and Kellermann, W. (**2009**). "Design of robust superdirective beamformers as a convex optimization problem," in *Proceedings of the IEEE International Conference on Acoustics, Speech, and Signal Processing (ICASSP)*, pp. 77–80.

Mathews, C. P., and Zoltowski, M. D. (**1994**). "Eigenstructure techniques for 2-D angle estimation with uniform circular arrays," IEEE Trans. Signal Process. **42**, 2395–2407.

Meyer, J. (**2001**). "Beamforming for a circular microphone array mounted on spherically shaped objects," J. Acoust. Soc. Am. **109**, 185–193.

Rafaely, B. (**2005**). "Analysis and design of spherical microphone arrays," IEEE Trans. Audio Speech Lang. Process. **13**, 135–143.

Uzkov, A. I. (**1946**). "An approach to the problem of optimum directive antenna design," Comp. Rendus (Doklady) de l'Acad. Sci. de l'URSS **LIII**, 35–38.

Ward, D. B., Williamson, R. C., and Kennedy, R. A. (**1998**). "Broadband microphone arrays for speech acquisition," Acoust. Austral. **26**, 17–20.

Yan, S., and Ma, Y. (**2005**). "Robust supergain beamforming for circular array via second-order cone programming," Appl. Acoust. **66**, 1018–1032.

Yan, S., Sun, H., Ma, X., Svensson, U. P., and Hou, C. (**2011**). "Time-domain implementation of broadband beamformer in spherical harmonics domain," IEEE Trans. Audio Speech Lang. Process. **19**, 1221–1230.

Zhao, L., Benesty, J., and Chen, J. (**2014**). "Design of robust differential microphone arrays," IEEE Trans. Audio Speech Lang. Process. **22**, 1455–1466.